Int. J. Solids Structures Vol. 25, No. 4, pp. 393–405, 1989
Printed in Great Britain.

0020-7683/89 $3.00 + .00

TRANSIENT GENERALIZED FORCES DUE TO DISLOCATION ARRAY–GROWING CRACK INTERACTION

L. M. BROCK and J.-S. WU
Department of Engineering Mechanics, University of Kentucky, Lexington, KY 40506, U.S.A.

(*Received* 18 *February* 1988; *in revised form* 2 *September* 1988)

Abstract—For insight into the dynamic interaction between growing cracks and dislocations during fracture, the dislocation forces and the crack driving force due to the dislocations themselves are calculated for a Mode III crack initially in equilibrium with a stationary array of screw dislocations. The calculations are based on the exact closed-form solution for a single, arbitrarily-placed, screw dislocation and a crack growing at a largely arbitrary speed. They show that, in the absence of an applied stress in the material, the dislocation has no tendency to follow the crack edge as it moves but is, instead, attracted to the crack surface. If the dislocation is a member of an array, however, it can either be attracted to or repulsed by the crack surface, and could very well follow the crack edge by jogging. More generally, both the dislocation and crack driving forces exhibit dynamic effects embodied in the crack edge speed, and undergo rapid changes at fracture initiation, especially if the crack instantaneously attains a finite speed.

1. INTRODUCTION

Rice and Thomson (1974), Li (1981) and Ohr (1985) have studied the role of dislocation emission from crack edges in the prediction and characterization of fracture, while Majumdar and Burns (1981) and Thomson and Sinclair (1982) have studied the dislocation-induced shielding of crack edges from applied stresses. These studies demonstrate the importance of crack–dislocation interaction in fracture mechanics.

The studies are based, however, on quasi-static analyses, so that detailed information on the order of fracture events and their rates of occurrence is often not possible. Moreover, the studies may not accurately describe fracture under dynamic loading, with its associated wave propagation effects (Achenbach, 1973). To extend these studies, therefore, to dynamic situations, the screw dislocation motion near a crack which begins to grow in Mode III upon the diffraction of a plane *SH*-wave was analyzed (Brock and Jolles, 1987). The analysis was based on approximations of formally exact transient solutions, and presumed that the dislocations migrate toward the moving crack edge.

This presumption gave results which seemed to agree qualitatively with aspects of damage zone geometry observed near crack edges. It was based on a result of quasi-static generalized force analysis, e.g. Rice and Thomson (1974), that a dislocation in the absence of applied stresses and other boundaries will be attracted to a crack surface. Moreover, it relied on the observation (Hirth and Lothe, 1982) that dislocations may well undergo jogging from one glide plane to another during motion.

However, the analysis in Brock and Jolles (1987) did not determine what the actual generalized forces were during the crack growth process. The purpose of this article is, therefore, to move an important step beyond that analysis and examine the transient generalized forces due to the interaction between a growing crack and a stationary screw dislocation array. Both dislocation forces and the crack driving force J are considered and, moreover, the analysis will be exact. The first step in the analysis is taken in the next section, where a general problem is stated, and its formal solution given.

2. GENERAL PROBLEM AND ITS FORMAL SOLUTION

Figure 1 shows a semi-infinite crack defined in the x–y plane as $y = 0$, $x < 0$. For $s < 0$, where s = (rotational wave speed) × (time), the crack is at rest near a right-handed

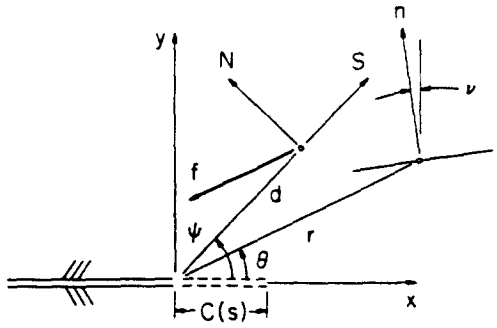

Fig. 1. Geometry for a single dislocation.

screw dislocation of Burgers vector magnitude b. The polar coordinates (r, θ) of the dislocation are $(d > 0, 0 \leqslant \psi < \pi/2)$, and the glide plane extends into the crack edge. For $s > 0$, the crack grows in Mode III along the x-axis, so that its edge is located at $y = 0$, $x = C(s)$. Here C is continuous and single-valued, $C(0) = 0$, $0 \leqslant \dot{C} < 1$, $s \geqslant 0$ and $\dot{}$ denotes s-differentiation. The inequalities preclude crack edge retreat and supersonic speeds.

The process can be viewed as the superposition of crack–dislocation and applied stress–crack interaction processes. Our interest is chiefly in the former, and so we restrict attention to the governing equations for it: when $s > 0$

$$\nabla^2 w + \frac{b}{\mu}\delta'(N)H(-S)H(S+d) - \ddot{w} = 0, \qquad w(\mathbf{x}, 0^+) = w_0(\mathbf{x}) \tag{1a,b}$$

for all $\mathbf{x}$ except $y = 0$, $x < C$, where

$$s_y = 0. \tag{2}$$

In eqns (1) $w(\mathbf{x}, s)$ and $w_0(\mathbf{x})$ are the antiplane displacements for $s > 0$ and $s < 0$, respectively, and $\mathbf{x} = (x, y)$ is the position vector of points in the plane, while

$$s_x = \mu\frac{\partial w}{\partial x}, \qquad s_y = \mu\frac{\partial w}{\partial y} \tag{3}$$

are the only non-zero tractions. The coordinates (S, N) are aligned with the dislocation glide plane, as indicated in Fig. 1. The parameter μ is the shear modulus, ∇^2 the Laplacian operator, and the non-homogeneous term in eqn (1a) is the Burridge–Knopoff (1964) equivalent body-force representation for the screw dislocation. The symbols δ and H denote the Dirac and Heaviside functions, and $(\,)'$ signifies differentiation with respect to the argument.

By superposition, the solution of eqns (1)–(3) can be written as

$$w = w_0 + W \tag{4}$$

where w_0 is as defined above, and W for $s > 0$ satisfies the conditions

$$\nabla^2 W - \ddot{W} = 0, \qquad W(\mathbf{x}, 0^+) = 0 \tag{5}$$

for all $\mathbf{x}$ except $y = 0$, $0 < x < C$, where

$$S_y = -s_{y0}. \tag{6}$$

The previously-introduced function w_0 is, of course, the equilibrium solution existing for $s < 0$, and has been obtained by Majumdar and Burns (1981) as

$$\frac{2\pi}{b} w_0 = \text{Im ln}\left(\frac{\sqrt{z}+\sqrt{D}}{\sqrt{z}-\sqrt{\bar{D}}}\right), \qquad z = r\,e^{i\theta}, \qquad D = d\,e^{i\psi} \tag{7}$$

by using conformal mapping techniques. Here ($\bar{}$) denotes the complex conjugate. The function W, then, must be the displacement arising from the removal of the w_0-induced traction by the growing crack. Standard Green's function (Carrier and Pearson, 1976) methods give for $\pm y < 0$ the formal solution of eqns (5)

$$\pm W = \frac{1}{\mu\pi}\int\int \frac{dp\,dq}{\sqrt{[(s-q)^2-(x-p)^2-y^2]}} S_y(p,0,q) \tag{8}$$

where the variables $(p, 0, q)$ correspond to (x, y, s). The integration area is that portion of the p–q plane where both the argument of the radical is positive and S_y along $y = 0$ does not vanish. By following Achenbach (1970), it can be shown that S_y along $y = 0$ is given by eqn (6) when $0 < x < C$, by the relation

$$S_y = \frac{1}{\pi\sqrt{(\eta-K)}}\int_{\xi}^{K} d\upsilon \frac{\sqrt{(K-\upsilon)}}{\eta-\upsilon} s_{y0}\left(\frac{\upsilon-\xi}{\sqrt{2}}, 0, \frac{\upsilon+\xi}{\sqrt{2}}\right) \tag{9}$$

when $C < x < s$, and vanishes otherwise. Here (ξ, η) are the characteristic variables

$$\sqrt{2}\xi = s-x, \quad \sqrt{2}\eta = s+x \tag{10}$$

and $\eta = K(\xi)$ defines the ξ–η plane trajectory of the crack edge, i.e.

$$K-\xi = \sqrt{2}C\left(\frac{K+\xi}{\sqrt{2}}\right). \tag{11}$$

The contour $\eta = \xi$ defines the original crack edge position $x = 0$.

While an exact solution, the formal assembly implied by eqn (4) is inconvenient both for purposes of studying solution behavior, and for obtaining the results intended here. The analysis of Brock and Jolles (1987) encountered a similar situation, and derived more explicit results valid for $r/d \ll 1$, i.e. in the neighborhood of the initial crack edge location. By following the transient analysis for a concentrated force near a stationary crack (Brock, 1986), the procedures used by Brock and Jolles (1987) can, in fact, be applied here to yield more explicit results which are, simultaneously, exact. This application begins in the next section with the expression for S_y.

3. SIMPLIFICATION OF S_y

Differentiation of eqn (7) gives

$$s_{y0} = A_0, \qquad \frac{2\pi}{\mu b} A_0 = \sqrt{\left(\frac{d}{x}\right)} \frac{(x-d)\cos\tfrac{1}{2}\psi}{(x-d\cos\psi)^2+d^2\sin^2\psi} \tag{12}$$

for $y = 0, x > 0$. Substitution of eqn (12) into eqn (9) in light of eqn (10) and the integration variable change $\sqrt{2}\upsilon = s-x-2u$ then yields the integral

$$\frac{2\pi}{\mu b}S_y = -\frac{1}{\pi\sqrt{(x-C_1)}}\sqrt{d}\cos\frac{1}{2}\psi\int_{-C_1}^{0}du\sqrt{\left(\frac{u+d}{u+x}\right)}\sqrt{\left(\frac{u+C_1}{-u}\right)}\frac{1}{(u+d\cos\psi)^2+d^2\sin^2\psi} \tag{13}$$

where C_1 satisfies the implicit relations

$$C_1 = C(s_1), \qquad s_1 - C_1 = s - x. \tag{14}$$

The integration in eqn (13) lies along the branch cut $-C_1 < u < 0$ of the integrand, which itself exhibits simple poles at $u = -x < 0$ and $u = -d\,e^{\pm i|\psi|}$ and vanishes as $O(u^{-2})$ when $|u| \to \infty$. Cauchy residue theory can, therefore, be employed, and it is easily shown that eqn (13) can be rewritten as

$$s_y = -A_0 + A, \qquad \frac{2\pi}{\mu b}A = \sqrt{\left(\frac{d_1}{x-C_1}\right)}\frac{x\cos\frac{1}{2}\psi_1 - d\cos(\frac{1}{2}\psi_1 - \psi)}{(x-d\cos\psi)^2+d^2\sin^2\psi} \tag{15}$$

for $y = 0$, $C_1 < x < s$, where (d_1, ψ_1) defined as

$$D - C_1 = d_1\,e^{i\psi_1} \tag{16}$$

are the polar coordinates of the dislocation with respect to the crack edge position $y = 0$, $x = C_1$. It is noted that $(d_1, \psi_1) = (d, \psi)$, and thus $A = A_0$, when $C_1 = 0$, i.e. $s_1 = 0$. With eqns (15) in hand, the formal integration (8) can now be carried out.

4. SIMPLIFICATIONS OF W

In view of their ranges of definition, it is readily shown that the regions of integration in the p–q plane arising from the substitution of eqns (6), (12) and (15) into eqn (8) have the general form indicated in Fig. 2. There it is noted that, in terms of the more convenient integration variables

$$\sqrt{2u} = q - p, \qquad \sqrt{2v} = q + p \tag{17}$$

corresponding to (ξ, η), the regions can be located in terms of the contours $v = u$, $v = K(u)$ and $v = M(u)$. The first two were defined earlier in terms of (ξ, η) ; the third contour locates the upper boundary of the area in which the argument of the radical in eqn (8) is positive, i.e.

$$\sqrt{2M} = s + x - \frac{y^2}{s - x - \sqrt{2u}}, \qquad |y| \neq 0. \tag{18}$$

Upon making variable changes (17), it can be shown in view of Fig. 2 that

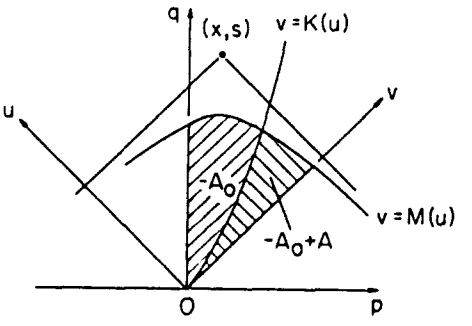

Fig. 2. Schematic of integration regions for W.

$$\pm\sqrt{2}\frac{\pi}{\mu}W=\int_0^{u^*}\frac{\mathrm{d}u}{\sqrt{(\xi-u)}}\int_K^M\frac{A\,\mathrm{d}v}{\sqrt{(M-v)}}-\int_0^{u_0}\frac{\mathrm{d}u}{\sqrt{(\xi-u)}}\int_u^M\frac{A_0\,\mathrm{d}v}{\sqrt{(M-v)}} \tag{19}$$

for $\pm y<0$, where $u=u_0$ defines the intersection of the contours $v=u$ and M, and is given by

$$u_0=s-r \tag{20}$$

while $u=u^*$ defines the intersection of the contours $v=K$ and M, and therefore satisfies the implicit relations

$$\sqrt{2u^*}=s-C^*-r^*,\qquad C^*=C(s^*),\qquad s^*=s-r^* \tag{21a}$$

where (r^*,θ^*) defined by

$$z-C^*=r^*\,\mathrm{e}^{\mathrm{i}\theta^*} \tag{21b}$$

are the polar coordinates of x with respect to the crack edge location $y=0$, $x=C^*$. It is easily shown that $u_0\geqslant u^*$. Employing eqns (15) and (17) to write the first v-integration in eqn (19) more explicitly gives

$$\frac{b}{\pi}\frac{\sqrt{d_1}}{2^{1/4}}\int_K^M\frac{\mathrm{d}v}{\sqrt{(M-v)}\sqrt{(v-K)}}\,\frac{(v-u)\cos\tfrac{1}{2}\psi_1-\sqrt{2d}\cos(\tfrac{1}{2}\psi_1-\psi)}{(v-u-\sqrt{2d}\cos\psi)^2+2d^2\sin^2\psi} \tag{22}$$

where it is noted that (d_1,ψ_1) are independent of v. This integration is along the branch cut $K<v<M$ of the integrand, which itself exhibits simple poles at $v=u+\sqrt{2d}\,\mathrm{e}^{\pm\mathrm{i}|\psi|}$ and behaves as $O(v^{-2})$ as $|v|\to\infty$. Cauchy residue theory can then again be used with the result that eqn (22) becomes

$$\frac{b}{\pi}\sqrt{(\xi-u)}\,\mathrm{Re}\,\frac{1}{\sqrt{[y^2+(x-D)^2-(s-D-\sqrt{2u})^2]}}. \tag{23}$$

Interestingly enough, the second v-integration in eqn (19) gives an identical result, so that eqn (19) reduces to

$$\pm\sqrt{2}\frac{\pi}{b}W=\mathrm{Re}\int_{u^*}^{u_0}\frac{\mathrm{d}u}{\sqrt{[y^2+(x-D)^2-(s-D-\sqrt{2u})^2]}} \tag{24}$$

which can be integrated to yield, cf. eqns (7),

$$\frac{4\pi}{b}W=\mathrm{Im}\,\ln\left(\frac{\sqrt{z}+\sqrt{D}}{\sqrt{z}-\sqrt{D}}\right)\left(\frac{\sqrt{\bar{D}}+\sqrt{z}}{\sqrt{\bar{D}}-\sqrt{z}}\right)\left(\frac{\sqrt{z^*}-\sqrt{D^*}}{\sqrt{z^*}+\sqrt{D^*}}\right)\left(\frac{\sqrt{\bar{D}^*}-\sqrt{z^*}}{\sqrt{\bar{D}^*}+\sqrt{z^*}}\right),\qquad s\geqslant r \tag{25}$$

where

$$z^*=r^*\,\mathrm{e}^{\mathrm{i}\theta^*},\qquad D^*=d^*\,\mathrm{e}^{\mathrm{i}\psi^*} \tag{26}$$

and (d^*,ψ^*) defined by

$$D-C^*=d^*\,\mathrm{e}^{\mathrm{i}\psi^*} \tag{27}$$

are the polar coordinates of the dislocation with respect to the crack edge location $y=0$,

$x = C^*$. With eqns (7) and (25) in hand, the general problem solution can now be used to study generalized forces. Dislocation forces are considered in the next section.

5. DISLOCATION FORCES

By means of the Peach–Koehler idea (Weertman and Weertman, 1964), the force per unit length acting on any segment of the dislocation can be obtained directly from the traction components. If one is interested in the antiplane traction acting on a plane the normal of which is in the n-direction, then the derivative of w with respect to n is required, and from eqns (7) and (25) it can be shown that

$$\frac{4\pi}{b}\frac{\partial w_0}{\partial n} = \mathrm{Re}\,\frac{e^{iv}}{\sqrt{z}}\left(\frac{1}{\sqrt{z}-\sqrt{D}} - \frac{1}{\sqrt{z}+\sqrt{\bar{D}}}\right) \tag{28a}$$

$$\frac{4\pi}{b}\frac{\partial W}{\partial n} = \mathrm{Re}\,\frac{e^{iv}}{(1-\dot{C}\cos\theta)^*}\cdot\frac{1}{z-D}\left[\sqrt{\left(\frac{D}{z}\right)}\left(1-\frac{\dot{C}}{2}(1+e^{i\theta})\right)+i\dot{C}\sqrt{\left(\frac{r}{D}\right)}\sin\frac{1}{2}\theta\right]^*$$
$$+\frac{1}{z-\bar{D}}\left[\frac{\sqrt{\bar{D}}}{\sqrt{z}}\left(1-\frac{\dot{C}}{2}(1+e^{i\theta})\right)+i\dot{C}\frac{\sqrt{r}}{\sqrt{\bar{D}}}\sin\frac{1}{2}\theta\right]^* - \mathrm{Re}\,\frac{e^{iv}}{\sqrt{z}}\left(\frac{\sqrt{D}}{z-D}+\frac{\sqrt{\bar{D}}}{z-\bar{D}}\right), \qquad s \geqslant r \tag{28b}$$

where, as seen in Fig. 1, v is the angle between the n- and y-directions. We also note that $z-D = z^*-D^*$, and that $\dot{C}$ is the crack speed nondimensionalized with respect to the rotational wave speed. Three force components are of particular interest, the component along the glide plane, f_S, and those in the coordinate direction, f_x and f_y. These components can be obtained from eqns (28a) and (28b) by setting $v = \psi$ for f_S, $v = 0$ for f_x and $v = -\pi/2$ for f_y, and then letting z approach D along normals to the particular component direction (Dundurs, 1968). The Peach–Koehler idea thereby yields

$$\frac{2\pi}{\mu b^2}f_S^0 = -\frac{1}{2d}, \quad \frac{2\pi}{\mu b^2}f_x^0 = -\frac{1}{2d}\cos^2\frac{1}{2}\psi, \quad \frac{2\pi}{\mu b^2}f_y^0 = -\frac{1}{4d}\tan\frac{1}{2}\psi\left(1+2\cos^2\frac{1}{2}\psi\right) \tag{29a–c}$$

while for $s \geqslant d$, i.e. after the arrival of the crack edge motion signal,

$$\frac{2\pi}{\mu b^2}F_S = \left(\frac{1}{d^*}-\frac{1}{d}\cos\psi^*\right)B^*\cos^2\frac{1}{2}\psi^*, \qquad B^* = \frac{1}{2}-\frac{1-\dot{C}^*}{1-\dot{C}^*\cos\psi^*} \tag{30a}$$

$$\frac{2\pi}{\mu b^2}F_x = \frac{1}{2d}\cos^2\frac{1}{2}\psi + \frac{B^*}{d^*}\cos^2\frac{1}{2}\psi^* \tag{30b}$$

$$\frac{2\pi}{\mu b^2}F_y = -\frac{1}{2d}\cos^2\frac{1}{2}\psi\cot\psi + \frac{B^*}{d^*}\left(\cot\psi^*-\tan\frac{1}{2}\psi\right)\cos^2\frac{1}{2}\psi^* \tag{30c}$$

where s^* is now defined by the implicit relation

$$s^* = s-d^*. \tag{31}$$

The explicit dependence of B^* on $\dot{C}^*$ shows that the transient analysis of dislocation forces does reveal dynamic effects. Indeed, the behaviour of B^* is clearly rather sensitive to values of $\dot{C}^*$. Equations (29) and (30) also show that, in view of eqn (27), the dislocation force components are generally inversely proportional to the initial crack edge–dislocation separation, d.

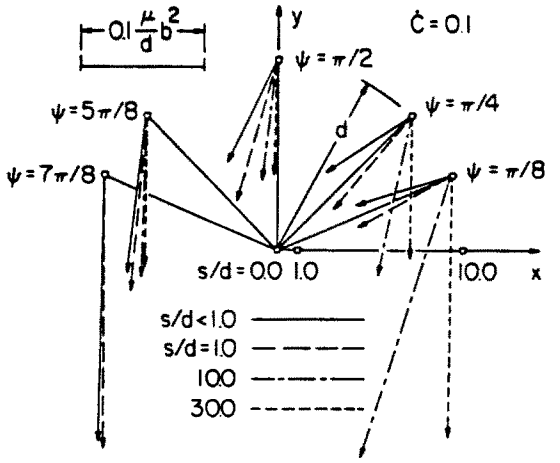

Fig. 3. Dislocation force for individual dislocations.

In Fig. 1 the resultant dislocation force f is shown schematically at an angle to the glide plane; this situation is, in fact, generally true, as can be confirmed by comparing f_S from eqns (29) to (31) with the resultant force magnitude

$$|f| = \sqrt{(f_x^2 + f_y^2)}. \tag{32}$$

To illustrate the behavior of f, its magnitude and orientation for individual dislocations with different values of ψ at various instants s are shown to scale in Fig. 3, where $\dot{C}$ is given the constant value 0.1. The points marked on the x-axis there indicate where the crack edge is at a given s. In Fig. 3, it is seen that f is always directed to points behind the crack edge and for $s/d \gg 1$, becomes perpendicular to the crack surface. That is, the dislocations never have any tendency to move with the crack edge, and they are eventually attracted directly to the crack surface. In terms of the component f_S, Fig. 3 shows that dislocations existing behind the crack edge ($|\psi| > \pi/2$) increase their tendency to move on the glide plane, while those ahead ($|\psi| < \pi/2$) see this tendency decrease.

It should also be noted that the arrival of the crack edge motion signal at $s = d$ causes jumps in both the magnitude and direction of f. However, eqns (30) show that these discontinuities disappear if the crack edge is allowed to accelerate from zero speed, i.e. $\dot{C}(0) = 0$.

6. CRACK DRIVING FORCE J

Rice (1968) has shown that for a Mode III crack, the generalized force J is given by

$$2\mu J = K_3^2 \tag{33}$$

where K_3 is the stress intensity factor. From eqns (28a), (28b) and (3) we find for all $s \geqslant 0$ that

$$\frac{2\pi}{b}\frac{\partial w_0}{\partial y} \approx -\frac{1}{\sqrt{(rd)}}\cos\frac{1}{2}\psi\cos\frac{1}{2}\theta (r \approx 0) \tag{34a}$$

$$\frac{2\pi}{b}\frac{\partial W}{\partial y} \approx -\frac{2\pi}{b}\frac{\partial w_0}{\partial y}(r \approx 0) \tag{34b}$$

$$\frac{2\pi}{b}\frac{\partial W}{\partial y} \approx \frac{\dot{C}^* - 1}{\sqrt{(rd)^*(1-\dot{C}\cos\theta)^*}}\cos\frac{1}{2}\psi^*\cos\frac{1}{2}\theta^* (r \approx C^*). \tag{34c}$$

From these results it follows that

$$\frac{\mu}{b}K_3 = -\frac{1}{\sqrt{(2\pi d)}}\cos\frac{1}{2}\psi(s=0^-), \quad -\sqrt{\left(\frac{1-\dot{C}}{2\pi d}\right)^*}\cos\frac{1}{2}\psi^*(s\geqslant 0). \tag{35}$$

Equation (35) indicates that, like the dislocation forces with their explicit dependence on $\dot{C}$, J exhibits a dynamic effect. Indeed, it is a continuous function of s only when $\dot{C}$ is continuous. Like the dislocation force, moreover, J is also generally inversely proportional to d.

With these observations and results available, we now consider the generalized forces associated with arrays of dislocations near the growing crack.

7. DISLOCATION ARRAYS—BASIC RESULTS

Consider in Fig. 4 the pair of right-handed screw dislocations which are located symmetrically about the crack plane at $(r,\theta) = (d, \pm\psi)$. From our previous results, it is easily shown that for this pair

$$\frac{2\pi}{b}\frac{\partial w_0}{\partial n} = \mathrm{Re}\frac{e^{i\nu}}{\sqrt{z}}\left(\frac{\sqrt{D}}{z-D}+\frac{\sqrt{\bar{D}}}{z-\bar{D}}\right) \tag{36a}$$

while for $s \geqslant r$

$$\frac{2\pi}{b}\frac{\partial W}{\partial n} = -\frac{2\pi}{b}\frac{\partial w_0}{\partial n} + \mathrm{Re}\frac{e^{i\nu}}{(1-\dot{C}\cos\theta)^*}\cdot\frac{1}{z-D}\left[\sqrt{\left(\frac{D}{z}\right)}\left(1-\frac{\dot{C}}{2}(1+e^{i\theta})\right)\right.$$
$$\left.+i\dot{C}\sqrt{\left(\frac{r}{D}\right)}\sin\frac{1}{2}\theta\right]^* + \frac{1}{z-\bar{D}}\left[\frac{\sqrt{\bar{D}}}{\sqrt{z}}\left(1-\frac{\dot{C}}{2}(1+e^{i\theta})\right)+i\dot{C}\frac{\sqrt{r}}{\sqrt{\bar{D}}}\sin\frac{1}{2}\theta\right]^*. \tag{36b}$$

From these expressions, the dislocation force components for the dislocation at (d,ψ) are found to be

$$\frac{2\pi}{\mu b^2}f_s^0 = -\frac{1}{2d}, \quad \frac{2\pi}{\mu b^2}f_x^0 = -\frac{1}{d}\cos^2\frac{1}{2}\psi, \quad \frac{2\pi}{\mu b^2}f_y^0 = \frac{1}{2d}(\cot\psi - \sin\psi) \tag{37a-c}$$

and for $s \geqslant d$

$$\frac{2\pi}{\mu b^2}(F_s+f_s^0) = \frac{1}{2d^*(1-\dot{C}\cos\psi)^*}\left[\left(\frac{\dot{C}^*}{2}-1\right)\cos(\psi-\psi^*)+\frac{\sin(\psi-\psi^*)}{\sin\psi^*}\right.$$
$$\left.+\dot{C}^*\left(\frac{3}{2}\cos\psi^*-\frac{d^*}{d}\right)\right] \tag{38a}$$

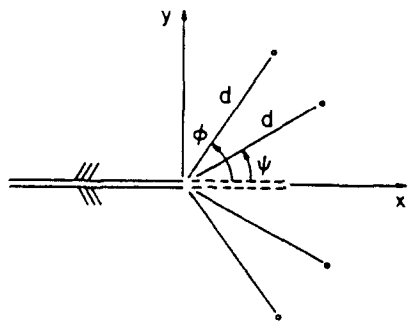

Fig. 4. Geometry for two symmetrically-arranged pairs of dislocations.

$$\frac{2\pi}{\mu b^2}(F_x+f_x^0)=\frac{1}{d^*(1-\dot{C}\cos\psi)^*}\left[\left(\frac{\dot{C}}{2}-1\right)\cos^2\frac{1}{2}\psi+\frac{\dot{C}}{2}\right]^* \tag{38b}$$

$$\frac{2\pi}{\mu b^2}(F_y+f_y^0)=\frac{1}{2d^*(1-\dot{C}\cos\psi)^*}\left[\left(\frac{\dot{C}}{2}-1\right)\sin\frac{1}{2}\psi+\frac{1}{\sin\psi}(\cos\psi-C)\right]^*. \tag{38c}$$

Referring again to Fig. 4, we now consider the force components on this same dislocation due to another pair of right-handed screw dislocations placed symmetrically about the crack plane at $(r,\theta)=(d,\pm\phi)$. Upon setting $z=de^{i\psi}$ and $D=de^{i\phi}$ in eqn (36), we find that for this pair eqns (37) are replaced by

$$\frac{2\pi}{\mu b^2}f_S^0=G_0(\psi)=0, \qquad \frac{2\pi}{\mu b^2}f_x^0=G_0(0), \qquad \frac{2\pi}{\mu b^2}f_y^0=-G_0(-\pi/2) \tag{39a–c}$$

while for $s\geqslant d$, eqns (38) become

$$\frac{2\pi}{\mu b^2}(F_S+f_S^0)=G_-(\psi,\psi)-G_-(\psi,\phi)+G_+(\psi,\psi)-G_+(\psi,-\phi) \tag{40a}$$

$$\frac{2\pi}{\mu b^2}(F_x+f_x^0)=G_-(0,\psi)-G_-(0,\phi)+G_+(0,\psi)-G_+(0,-\phi) \tag{40b}$$

$$\frac{2\pi}{\mu b^2}(F_y+f_y^0)=-G_-(-\pi/2,\psi)+G_-(-\pi/2,\phi)-G_+(-\pi/2,\psi)+G_+(-\pi/2,-\phi) \tag{40c}$$

where

$$2dG_0(v)=\frac{\cos(v+\frac{1}{2}(\phi-3\psi))-\cos(v-\frac{1}{2}(\phi+\psi))}{1-\cos(\phi-v)}+\frac{\cos(v-\frac{1}{2}(\phi+3\psi))-\cos(v+\frac{1}{2}(\phi-\psi))}{1-\cos(\phi+\psi)} \tag{41}$$

$$2d(1-\cos(\phi\pm\psi))(1-\dot{C}\cos\psi)^*G_\pm(v,\beta)=\sqrt{\left(\frac{h}{d}\right)^*}\left(1-\frac{\dot{C}^*}{2}\right)\cos\left(v-\beta+\frac{1}{2}(\phi\pm\psi)^*\right)$$
$$-\frac{\dot{C}^*}{2}\sqrt{\left(\frac{h}{d}\right)^*}\cos\left(v-\beta+\frac{1}{2}(\phi\mp\psi)^*\right)-\sqrt{\left(\frac{d}{h}\right)^*}\dot{C}^*\sin\frac{1}{2}\psi^*\sin\left(v-\beta\pm\frac{1}{2}\phi^*\right) \tag{42}$$

and (h^*,ϕ^*) defined by

$$de^{i\phi}-C^*=h^*e^{i\phi^*} \tag{43}$$

are the polar coordinates of $de^{i\phi}$ with respect to the crack edge location $y=0$, $x=C^*$.

A glance at eqn (39a) and comparison of eqn (37a) with (29a) shows that, in equilibrium, the glide plane force f_S on a dislocation is unaffected by the presence of other dislocations. Equations (40) and (42) demonstrate that, once crack edge motion is detected, however, all dislocation force components depend on the other dislocations.

In regard to J, it is clear from symmetry arguments that obtaining the asymptotic expressions corresponding to eqns (34) for eqns (36) and (37) would give for the dislocation pair at $(d,\pm\psi)$

$$\frac{\mu}{b}K_3 = -\sqrt{\left(\frac{2}{\pi d}\right)}\cos\frac{1}{2}\psi(s=0^-), \quad -\sqrt{\left(\frac{2}{\pi d}\right)^*}\sqrt{(1-\dot{C}^*)}\cos\frac{1}{2}\psi^*(s\geqslant 0). \tag{44}$$

8. CALCULATIONS FOR A UNIFORM ARRAY

We now generalize Fig. 4 to define an array of dislocations comprised of seven pairs of symmetrically-arranged right-handed screw dislocations. The pairs are located at identical distances d from the initial crack edge position, with polar angles $\psi = \pm k\pi/8$ ($k = 1,\ldots,7$). The total dislocation force components on any one dislocation in the array can, of course, be computed by adding eqns (37) and (38) for that particular ψ to the summation with respect to ϕ of eqns (39) and (40) over all other values of $\psi > 0$ in the array. In Fig. 5, the magnitude and direction of the total resultant force on five of the dislocations in the array are shown to a scale for $\dot{C} = 0.2$ and various values of s.

Figure 5 indicates that, in equilibrium, the individual members of the dislocation array are repulsed from the crack plane, unless they lie near $|\psi| = \pi/2$, i.e. the perpendicular through the crack edge. This state is altered greatly, however, by the arrival of the crack edge motion signals: the total resultant force magnitude decreases by nearly one order in some cases, and the force itself becomes less repulsive—or even attractive—with respect to the crack plane. As crack growth proceeds, the total force magnitude tends to increase again, and those dislocations lying initially behind the crack edge are again repulsed by the crack surface.

Comparison of Figs 3 and 5 indicates that dislocations in this array are more sensitive to crack edge motion, and that, as presumed by Brock and Jolles (1987), dislocations could very well migrate toward the moving crack edge by jogging, if appropriate glide planes were available. It should be noted, however, that the instantaneous variations in the total resultant force with the crack edge motion signal arrival stems from the discontinuous nature of $\dot{C}$, as noted earlier for single dislocation resultant forces.

Turning now to crack driving force, K_3, for the symmetric array would simply be a summation of eqn (44) over the values $\psi > 0$. To illustrate its behavior, we plot this sum vs $s \geqslant 0$ for various values of constant $\dot{C}$ in Fig. 6. There it is seen that K_3, and thus, J, decreases in magnitude as both s and $\dot{C}$ increase. This behavior implies that crack edge shielding (Majumdar and Burns, 1981; Thomson and Sinclair, 1982), due to dislocation arrays can be temporary. The aforementioned explicit dynamic effect is manifested here as a jump in K_3 at the instant of fracture initiation.

9. CALCULATIONS FOR A STRESS-CONSISTENT ARRAY

The array considered above is uniform in the sense that only right-handed screw dislocations are present. If a symmetric array centered on the crack edge were, in fact, to

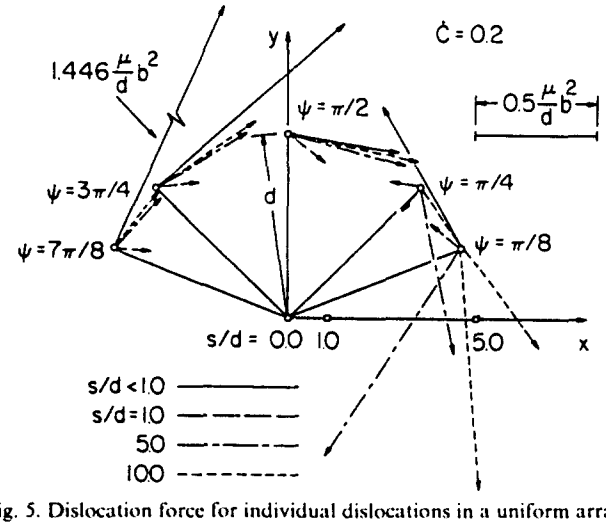

Fig. 5. Dislocation force for individual dislocations in a uniform array.

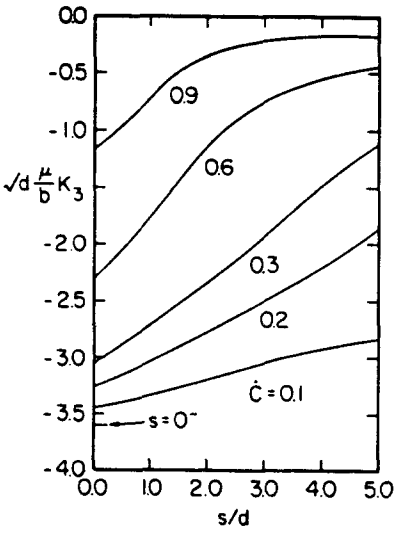

Fig. 6. Stress intensity factor response for a uniform array.

be generated by an antisymmetric antiplane stress field, then it is likely that the Burgers vectors for dislocations on opposite sides of the crack edge, i.e. opposite sides of $|\theta| = \pi/2$, would be in opposite directions. By altering the sign of b appropriately, eqns (37)–(40) and (44) can be used to describe the generalized forces for such an array. Thus, in Figs 7 and 8, we present analogies to Figs 5 and 6 for a symmetric array of six dislocation pairs with polar angles $\phi = \pm k\pi/8$ ($k = 1, \ldots, 7; k \neq 4$), where the dislocation pairs located behind the crack edge ($|\psi| > \pi/2$) are left handed.

In Fig. 7, dislocations nearer the crack plane are seen to be repulsed from it prior to the crack edge motion signal arrival, but attracted to it further away. The signal arrival then causes pronounced changes in both the magnitude and direction of the total resultant dislocation force: dislocations lying in front of the crack appear to be attracted to the moving crack edge, while those behind are eventually attracted to the crack surface.

Comparison of Figs 6 and 8 indicates that the general behavior of K_3, and thus, J, is largely the same for both arrays when $s/d > 1$. For $s/d > 1$, however, J actually increases slightly with both s and $\dot{C}$.

10. BRIEF DISCUSSION

This article examined the generalized forces due only to the interaction between a growing crack and a stationary array of screw dislocations. The force expressions were

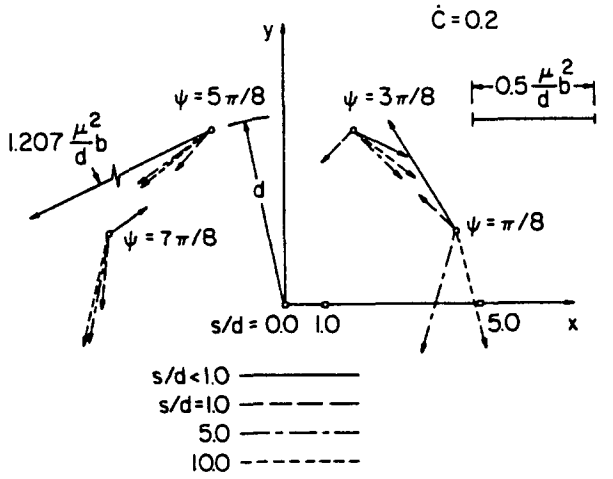

Fig. 7. Dislocation force for individual dislocations in a stress-consistent array.

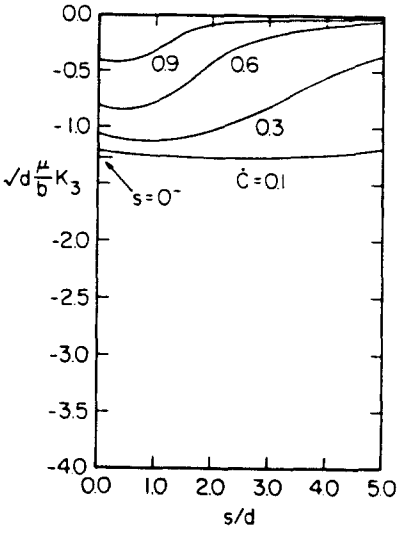

Fig. 8. Stress intensity factor response for a stress-consistent array.

based on exact solutions to the transient problem for a single screw dislocation. Study of the dislocation force components in this problem indicated that in the absence of an applied stress, an isolated screw dislocation is ultimately attracted to the crack surface, yet has no tendency to follow the moving crack edge. For two types of symmetrically-arranged dislocation arrays, however, individual members of the array can be attracted to the crack edge or repulsed from the crack surface. In both cases, the explicit dependence of the force components on the non-dimensionalized crack edge speed indicated a dynamic effect in the interaction process. Moreover, if the crack edge instantaneously achieves a finite speed, then the signals of this event cause instantaneous, and sometimes pronounced, changes in the dislocation force components.

An auxiliary of this signal arrival behavior of some interest in its own right was that the glide plane force on a screw dislocation in an array at rest near a stationary crack is independent of any other members of the array. This is no longer true when the crack edge motion signal arrives.

These results imply that the presumption of dislocation array migration toward a moving crack edge employed in the approximate dislocation–crack interaction analysis by Brock and Jolles (1987) has validity. More generally, the results indicate that, if alternate glide planes are available, and the dislocation force components can overcome the lattice friction (Bilby *et al.*, 1963; Shaw, 1984), then crack growth can indeed cause dislocation motion by jogging.

The study of the dynamic stress intensity factor which was needed for calculation of the crack driving force J showed that there was also an explicit dynamic effect, and that J is inversely related to both crack speed and time after crack motion initiation occurs. In regard to the factor itself, the study showed that crack edge shielding by the dislocation arrays considered can be temporary.

As mentioned at the outset, this article was an important step beyond the work of Brock and Jolles (1987). It was, obviously, based on presumed dislocation–crack kinematics and a rather idealized situation, because the equilibrium stress state generated by the stationary dislocations was assumed to be, without knowledge of an applied stress, sufficient to initiate fracture, and no fracture/dislocation motion criteria were actually invoked. Moreover, only quantities associated with crack–dislocation interaction, not with applied stress–crack interaction, were examined. Nevertheless, the observations made here will enable a study now ongoing to consider more realistic situations, in which the kinematics is viewed as the result of an applied stress and the material properties.

Acknowledgement—This research was supported by NSF Grant MEA8319605.

REFERENCES

Achenbach, J. D. (1970). Extension of a crack by a shear wave. *Z. Angew. Math. Phys.* **21**, 887–900.

Achenbach, J. D. (1973). *Wave Propagation in Elastic Solids*. North-Holland/American Elsevier, Amsterdam.

Bilby, B. A., Cottrell, A. H. and Swinden, K. H. (1963). The spread of plastic yield from a notch. *Proc. R. Soc.* **A272**, 304–314.

Brock, L. M. (1986). Transient dynamic Green's functions for a cracked plane. *Q. Appl. Math.* **44**, 265–275.

Brock, L. M. and Jolles, J. (1987). Dislocation–crack edge interaction in dynamic fracture and crack propagation. *Int. J. Solids Structures* **23**, 607–619.

Burridge, R. and Knopoff, L. (1964). Body force equivalents for seismic dislocations. *Bull. Seism. Soc. Am.* **54**, 1875–1888.

Carrier, G. F. and Pearson, C. E. (1976). *Partial Differential Equations*. Academic Press, New York.

Dundurs, J. (1968). Elastic interaction of dislocations with inhomogeneities. In *Mathematical Theory of Dislocations*. ASME, New York.

Hirth, J. P. and Lothe, J. (1982). *Theory of Dislocations*, 2nd Edn. Wiley-Interscience, New York.

Li, J. C. M. (1981). Dislocation sources. In *Dislocation Modelling of Physical Systems*. Pergamon Press, New York.

Majumdar, B. S. and Burns, S. J. (1981). An elastic theory of dislocations, dislocation arrays and inclusions near a sharp crack. *Acta Metall.* **29**, 579–588.

Ohr, S. M. (1985). An electron microscope study of crack tip deformation and its impact on the dislocation theory of fracture. *Mater. Sci. Engng* **72**, 1–35.

Rice, J. R. (1968). A path independent integral and the approximate analysis of strain concentration by notches and cracks. *ASME J. Appl. Mech.* **35**, 379–386.

Rice, J. R. and Thomson, R. (1974). Ductile versus brittle behaviour of crystals. *Phil. Mag.* **29**, 73–97.

Shaw, M. C. (1984). A critical review of mechanical failure criteria. *ASME J. Engng Mater. Technol.* **106**, 219–226.

Thomson, R. and Sinclair, J. E. (1982). Mechanics of cracks screened by dislocations. *Acta Metall.* **30**, 1325–1334.

Weertman, J. and Weertman, J. R. (1964). *Elementary Dislocation Theory*. Macmillan, New York.